Bioelectrochemistry 137 (2021) 107634

Contents lists available at ScienceDirect

Bioelectrochemistry

journal homepage: www.elsevier.com/locate/bioelechem

An electrochemical impedimetric sensing platform based on a peptide aptamer identified by high-throughput molecular docking for sensitive L-arginine detection

Yumin He [a,c], Li Zhou [b], Lei Deng [d], Zemeng Feng [a,*], Zhong Cao [b], Yulong Yin [a,c]

[a] Hunan Provincial Key Laboratory of Animal Nutritional Physiology and Metabolic Process, Key Laboratory of Agro-ecological Processes in Subtropical Region, Institute of Subtropical Agriculture, Chinese Academy of Sciences, National Engineering Laboratory for Pollution Control and Waste Utilization in Livestock and Poultry Production, Hunan Provincial Engineering Research Center for Healthy Livestock and Poultry Production, Scientific Observational and Experimental Station of Animal Nutrition and Feed Science in South-Central, Ministry of Agriculture, Changsha, Hunan 410125, PR China

[b] Collaborative Innovation Center of Micro/Nano Bio-sensing and Food Safety Inspection, Hunan Provincial Key Laboratory of Materials Protection for Electric Power and Transportation, School of Chemistry and Biological Engineering, Changsha University of Science and Technology, Changsha, Hunan 410004, PR China

[c] Animal Nutrition and Human Health Laboratory, College of Life Sciences, Hunan Normal University, Changsha, Hunan 410081, PR China

[d] School of Computer Science and Engineering, Central South University, Changsha 410075, PR China

ARTICLE INFO

Article history:
Received 28 May 2020
Received in revised form 12 August 2020
Accepted 12 August 2020
Available online 14 August 2020

Keywords:
Peptide aptamer
Docking
L-Arg
Biosensor
EIS
Isothermal titration calorimetry

ABSTRACT

As a primary building block for protein synthesis, L-arginine (L-Arg) is also a precursor for the synthesis of important metabolites, and is involved in various physiological and pathophysiological processes. L-Arg is a potential biomarker in clinical diagnosis and nutritional status assessment, making it valuable to quantify and monitor this biomolecule. In this study, peptide aptamers that specifically interact with L-Arg were identified by high-throughput molecular docking, and the binding capacities between the synthesized peptide aptamers and L-Arg were then measured by isothermal titration calorimetry. We hypothesized that the peptide aptamer with the greatest binding capacity could be used as the recognition element in a biosensor. A chemosynthetic peptide aptamer modified with mercaptan and spacer units (thioctic acid-GGGG-FGHIHEGY) was thus used to construct label-free electrochemical impedimetric biosensors for L-Arg based on gold electrodes. The optimum biosensor showed good sensitivity to L-Arg with a linear range of 0.1 pM–0.1 mM, and the calculated limit of detection (three times the signal-to-noise ratio) was 0.01 pM. Interference studies and assays of diluted serum samples were also carried out, and satisfactory results obtained. In conclusion, a potential method of peptide aptamer screening and biosensor fabrication for detecting small biological molecules was demonstrated.

1. Introduction

As a crucial amino acid, L-arginine (L-Arg) is a precursor for important metabolites such as polyamines, creatine, agmatine and some other amino acids including L-glutamine (L-Gln) and L-proline (L-Pro) [1]. L-Arg is also involved in various physiological and pathophysiological processes [2–7], and is the immediate precursor of nitric oxide, variously involved in the regulation of cell metabolism, insulin signaling and secretion, neurotransmission, and immune function [8,9]. The L-Arg concentration in serum ranges from 5 to 55 μM, and L-Arg has been regarded as an effective mediator for blood pressure management [3,10], as well as a potential biomarker in clinical diagnosis [11,12] and nutritional status assessment [13–15]. Thus, the quantification and monitoring of L-Arg is of high potential relevance.

High-performance liquid chromatography (HPLC), amino acid analyzer and capillary electrophoresis are traditional methods for the measurement of total amino acids, including L-Arg, as part of a single array, but the tedious sample preconditioning, time-consuming detection, and the cost of apparatus have limited their popularity [16]. Moreover, because L-Arg has no aromatic group, it is not feasible to directly detect L-Arg *via* label-free fluorescence.

A biosensor is a self-contained, integrated device that is capable of providing specific quantitative or semi-quantitative analytical information based on a biological element [17], enabling the fast measurement of small biomolecules. Nowadays, biosensors based on optical, surface plasmon resonance (SPR) have the merits of high sensitivity and selectivity [18], but the demand for labeling and a rather troublesome fabrication process has impeded their wider application. Moreover, potential toxic effects may be

* Corresponding author.
E-mail address: fengzemeng@isa.ac.cn (Z. Feng).

https://doi.org/10.1016/j.bioelechem.2020.107634
1567-5394/

brought about by fluorochrome modification [19]. In contrast, electrochemical biosensors represent an emerging advance in rapid, cost-effective, and sensitive biosensor fabrication, as the amount of the target can be inferred indirectly from changes at the electrode surface [20–22]. Since White and coworkers first brought L-lysine-decarboxylase into use as a biorecognition element, sensors of this construction [23], known as enzyme electrodes, have been increasingly used to detect amino acids. To date, the majority of L-Arg sensors have been designed with the aid of arginase and urease, where these enzymes catalyze the hydrolysis of L-Arg to ammonium and bicarbonate ions, allowing ammonia gas electrodes, ammonium ion-selective electrodes (ISEs), and/or glassy carbon electrodes (GCEs) to detect L-Arg indirectly [24]. However, the existing enzyme electrodes are confronted with major challenges due to the instability of enzymes, which leads to a cumulative loss of activity, enzymes leakage from the electrode is also a problem. A number of immobilization techniques have been tried, such as crosslinking with glutaraldehyde, which can help protect enzymes from leakage when the enzymes are non-covalently immobilized [25], and immobilization on porous supports; however, methods of retaining the activity, stability, and selectivity of enzymes are highly desired [26].

Aptamer-based biosensors possess better specificity and stability than enzyme electrodes [27,28]. Various oligonucleotides or short peptides, known as nucleic acid aptamers and peptide aptamers, can specifically recognize targets through their molecular properties [29–31]. Nucleic acid aptamers are generally selected through the systematic evolution of ligands by exponential enrichment (SELEX) [32]. The approaches to screening peptide aptamers can be summarized as *in vivo* screening, *in vitro* display, random peptide library, and molecular docking [29,33]. Both SELEX and the conventional methods used in aptamer screening are labor intensive, in that multiple steps are required, including binding and elution, and this circular process can repeat for 7–8 rounds, which is tedious and time-consuming [32]. *In silico* modeling has been adopted as an efficient strategy, which frees researchers from the tedious process of experimentally screening aptamers for electrochemical biosensors [34]. However, the yield ratio highly depends on the docking accuracy, thus subsequent experimental verification is necessary to eliminate false positive hits. Isothermal titration calorimetry (ITC) and SPR are the most reliable methods for verifying the molecular binding affinities predicted by docking. Generally, SPR is limited to validating the binding affinity of relatively large molecules (>1000 Dalton) due to the difficulty of immobilizing small targets [35].

A number of biosensors based on aptamers have been designed to recognize amino acids, including L-tryptophan (L-Trp) and L-phenylalanine (L-Phe) [36,37], as well as L-Arg [38,39]. However, the instability of RNA aptamers is a concern. An aptamer-based biosensor has also been designed to detect L-Arg by fluorescence labeling [40], which correctly distinguished between Arg enantiomers; however, fluorescent tags can have a potentially disruptive influence during the recognition process. Electrochemical impedance spectroscopy (EIS) is a label-free and nondisruptive technique based on the conformational changes of aptamers on an electrode in response to the target molecule. This response can be easily measured *via* the charge transfer resistance (*R*ct), and visualized in the form of a Nyquist plot [41]. Sensors based on EIS are low cost and simple to fabricate, and allow the rapid quantification of metal ions, biological molecules, other chemicals, and even whole cells [42–44]. The simplicity of fabricating EIS-based biosensors stems from the lack of a need for labeling and signal enhancement strategies.

In this study, we screened peptide aptamers by molecular docking and verified their activity by ITC, then selected the optimal peptide aptamer to construct a biosensor. The resulting EIS-based "aptasensor" exhibited good sensitivity and selectivity. This demonstrates the potential utility of docking, in combination with ITC validation, as a strategy to screen aptamers for the construction of biosensors for small molecules.

2. Materials and methods

2.1. Reagents

The peptide aptamers predicted by docking were chemically synthesized by Genescript Biotechnology Co., Ltd. (Nanjing, China) for ITC analysis (purity > 95%). The peptide aptamer with the greatest binding capacity, modified at the N-terminal with thioctic acid and a spacer unit (-GGGG-) (purity > 95%), was synthesized by China Peptides Co., Ltd. (Shanghai, China). $K_4[Fe(CN)_6]$, $K_3[Fe(CN)_6]$, potassium chloride (KCl), tris-(2-carboxyethyl) phosphine hydrochloride (TCEP), L-tyrosine (L-Tyr), L-threonine (L-Thr), L-Pro, L-lysine (L-Lys), L-histidine (L-His), L-aspartic acid (L-Asp), L-serine (L-Ser), L-asparagine (L-Asn), L-Gln, L-glutamic acid (L-Glu), L-methionine (L-Met), L-cysteine (L-Cys), L-alanine (L-Ala), L-isoleucine (L-Ile), L-leucine (L-Leu), L-glycine (L-Gly), L-valine (L-Val), L-Phe, L-Trp, and L-Arg were purchased from Aladdin (Wuhan, China). Phosphate-buffered saline (PBS) tablets consisting of 1.8 mM of KH_2PO_4, 10 mM of Na_2HPO_4, 137 mM of NaCl, and 2.7 mM of KCl were purchased from Sangon Biotech (Shanghai, China). Sulfuric acid (H_2SO_4) was purchased from Sinopharm Chemical Reagent Co., Ltd (Shanghai, China). Ultrapure water (18.3 MΩ cm^{-1}, Millipore Milli-Q system (Bedford, MA, U.S.A.) was used throughout the experiments.

2.2. Docking and peptide property prediction

Eight-mer peptide aptamers were extracted from the protein sequences of four species: *Homo sapiens*, *Mus musculus*, *Rattus norvegicus*, and *Sus scrofa*. A total of 29,185 protein sequences of the four species were obtained from the UniProt database. A total of 2,854,481 peptide fragments were generated by scanning the protein sequences with a sliding window of eight amino acids. The build_seq.py script included in PyMol [45], was used to build α-helices for the eight-mer peptides, which were then used as the initial conformations for the molecular dynamic simulations. The simulations were performed to investigate the stability of the complexes of eight-mer peptides and L-Arg using AutoDock 4.2.6 [46]. Binding energy scores were obtained for all of the complexes. Potential peptide aptamers were chosen for further experimental verification from high to low according to the binding free-energy scores.

2.3. Binding verification between peptide aptamers and L-Arg

To evaluate whether the predicted peptide aptamers could actually specifically bind to L-Arg, ITC experiments were performed using a Nano-ITC system (TA Instruments, U.S.A.). Samples in solution were thoroughly degassed before the titration started. Then, a 1 mM solution of peptide in PBS was drafted into the injection needle and a 0.1 mM solution of L-Arg (in PBS) was loaded into a microcalorimeter. A reference cell was used in each experiment, containing PBS, with a heat capacity equal to the contents of the sample cell. The syringe was connected to the sample cell through a cannula and filled with 100 μL of titrant. The experiments were conducted with periodical injections using an injection interval of 250 s and stirring at 125 rpm. All experiments were performed at 37 °C, and the first injection of 4 μL was excluded from data

fitting to account for diffusional loss of titrant. The data analysis was performed according to a previous study [47].

2.4. Fabrication of peptide aptamer-based biosensors

Peptide aptamer-based sensors were fabricated according to the process described below. First, polycrystalline gold disk electrodes (diameter 2 mm) were successively physically polished by 1, 0.5, and 0.03 μm alumina slurry, and then ultrasonically cleaned with deionized water, ethanol, and deionized water for 5 min each, followed by being electrochemically roughed in 1 M of H_2SO_4 by potential scanning between −0.2 and 1.6 V until a stable cyclic voltammogram was obtained. After being thoroughly washed with deionized water, the electrodes were blow-dried. Then, a 7-μL droplet of thioctic acid and the spacer-unit-modified peptide (0.5 μM) was dropped onto each of the pre-treated electrodes. The peptide solution was previously conditioned for 1 h with 5 mM of TCEP to cleave the disulfide bonds and form sulfhydryl groups for covalent binding to the gold surface. The electrodes were incubated at room temperature in a high-humidity atmosphere for a certain time. Finally, the integrated peptide aptamer-based sensor was gently rinsed with deionized water and stored in PBS until use.

2.5. Electrochemical detection

A conventional three-electrode system was used, comprising a polycrystalline gold disk electrode (2 mm in diameter) as a working electrode, Ag|AgCl as a reference electrode, and platinum wire as a counter electrode. Polishing materials were purchased from Chenhua Instrument Co., Ltd. (Shanghai, China). All of the electrochemical measurements were carried out using a CHI760E workstation (CH Instruments, Shanghai) connected to a running system. Throughout the electrode fabrication process, cyclic voltammetry (CV) and EIS signals were recorded in 10 mM of PBS with 0.1 M of KCl in which 10 mM $[Fe(CN)_6]^{3-/4-}$ (Fe^{3+}: Fe^{2+} = 1:1) was used as electrochemical reporter. CV was recorded between −0.2 and −0.6 V, and the EIS spectra were recorded at equilibrium potential (open circuit potential) at 0.245 mV without bias voltage in the frequency range of 0.1 Hz–10 kHz with a 5 mV amplitude.

2.6. Serum collection and determination of free amino acids

Porcine serum samples were collected in centrifuge tubes with heparin sodium and stored for 1 h at 4 °C, then centrifuged at 3000 rpm for 10 min. Then, the supernatant was transferred to new centrifuge tubes and kept at −80 °C until use. All porcine serum samples were collected from healthy Duroc × Landrace × Yorkshire pigs weighing approximately 25 kg. The present study was carried out in accordance with the Chinese guidelines for animal welfare and experimental protocols and approved by the Animal Care and Use Committee of the Institute of Subtropical Agriculture, Chinese Academy of Sciences. The amino acid contents of the pig serum were quantified by HPLC (Agilent 1260) according to a previously reported method [48].

3. Results and discussion

3.1. Docking and binding capacity verification of peptides with L-Arg

Docking has been extensively applied to simulate the binding between proteins and ligands. This *in silico* method has flourished as a fast and labor-free strategy in drug design. In this study, we used docking to predict the potential interaction between L-Arg and the eight-mer peptide aptamers extracted from the protein sequences. In the process of simulation, potential peptide aptamers that bind not specifically to L-Arg were excluded to ensure specificity. Among the docking results, four peptides (P1-P4) were outstanding in terms of binding energy, showing a probable tendency to interact with L-Arg while not responding to other amino acids. These peptides' sequences and binding energies are listed in Table 1, together with their isoelectric points, hydrophobicity, and overall charge as predicted by an online tool accessible at http://www.tulane.edu/~biochem/WW/PepDraw/.

Because docking is not necessarily accurate, and the yield ratio highly depends on the docking accuracy [49], further verification of the binding capacity was necessary. ITC and SPR are regarded as the gold standard for molecular binding verification [35]. However, due to the difficulty of immobilizing micro-molecules (<1000 Dalton) for SPR binding, label-free microcalorimetry is favored [50]. Here, the peptide aptamers and L-Arg were dissolved directly in binding buffer then titrated using ITC. The peptide aptamers P1-P4 were synthesized with high purity (>95%) and then applied for binding verification, in which the natural characteristics including charge and conformation of the peptide aptamers and L-Arg were retained by using PBS as binding buffer. The binding reaction was carried out at a temperature of 37 °C, and the peptide aptamer concentration was set at 1 mM, which was 10-fold higher than that of L-Arg. After titration, the first data point was discarded to improve the fitting accuracy. The titration results showed that only P2 could in fact interact with L-Arg (Fig. 1), and the dissociation constant was 6.734×10^{-4} mol L^{-1}. In contrast, P1, P3, and P4 showed no evidence of binding to L-Arg (Fig. S1). These ITC results indicated the successful prediction of a binder for L-Arg, and P2 (FGHIHEGY) was chosen as the peptide to conduct further research.

3.2. Biosensor fabrication and electrochemical characterization

With this chosen peptide aptamer, we reasonably hypothesized that it may be used to construct a peptide-based electrochemical biosensor, in which the binding between the peptide and its target would measurably alter the properties of the peptide-modified electrode. Recently, specific peptides that can recognize targets of interest have aroused attention because of their potential to substitute enzymes and nucleic acid aptamers in target recognition. Peptides can be easily immobilized to a gold electrode by mercaptan modification, which creates an Au—S bond. In this study, we appended thioctic acid and spacer units to the N-terminal of the identified peptide to design our biosensor, and the finally sequence was thioctic acid-GGGG-FGHIHEGY (P5).

Traditional three-electrode systems have proven stable and convenient as sensors, and offer versatility through the measurement of both CV and EIS signals. In this study, electrochemical detection was performed using the three-electrode system described in Section 2.5. After being physically polished and chemically roughed by sulfuric acid (1 M), the pre-treated gold electrode was dried. Then, 7 μL of 0.5 μM P5 (in PBS), which had been preconditioned by 5 mM of TCEP for 1 h, was dropped onto the electrode. The electrode was then kept in a high-humidity atmosphere for a certain time to immobilize the peptide by the formation of Au—S bonds. The high-humidity environment ensured that solution evaporation was avoided despite the lengthy process (several hours). After being washed by deionized water to remove excess P5, the electrodes were immersed in PBS until use. EIS and CV measurements were recorded throughout the experiment to monitor the fabrication process (Fig. 2). PBS (10 mM) was used as the background electrolyte and ferri-ferrocyanide (10 mM) was used as the redox reporter. The EIS peak of the bare gold electrode was extremely small. After incubation with the peptide, the redox peak decreased evidently and the *R*ct increased considerably

Table 1
Predicted properties and binding energies of peptides.

Code	Sequence (N′-C′)	Isoelectric point	Hydrophobicity (kcal mol^{-1})	Charge	Binding energy (kcal mol^{-1})
P1	IDRYASEN	4.01	16.96	−1	−3.95
P2	FGHIHEGY	6.05	14.95	−1	−3.82
P3	GQAKVCTY	8.70	12.18	1	−3.80
P4	TQTGSSSS	5.30	12.16	0	−3.76

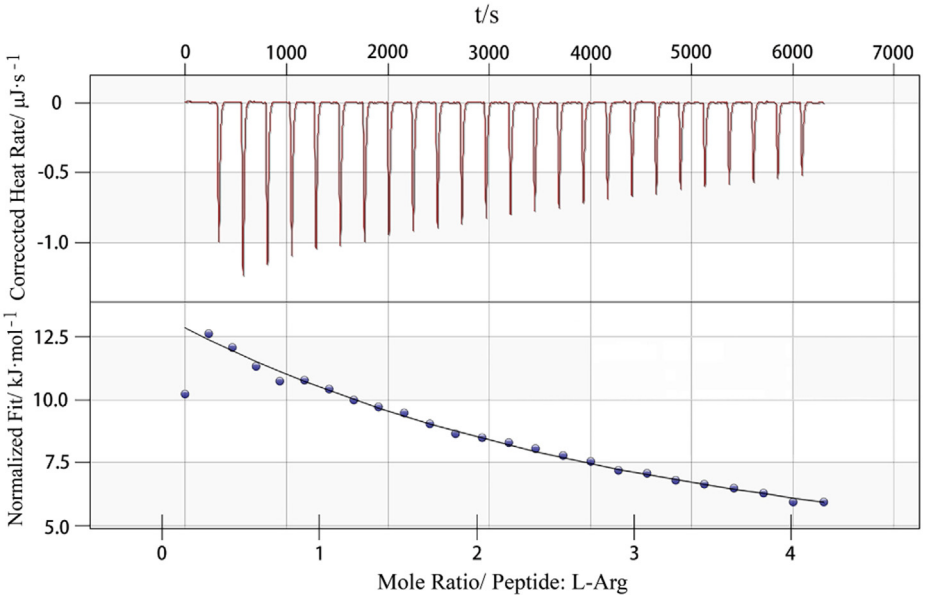

Fig. 1. ITC analysis of binding between P2 and L-Arg. P2 and L-Arg were separately dissolved in 10 mM of PBS, and 100 μL of P2 solution (1 mM) was titrated into a cell filled with 360 μL of L-Arg (0.1 mM), the volume of every drop being 4 μL. The first data point was discarded.

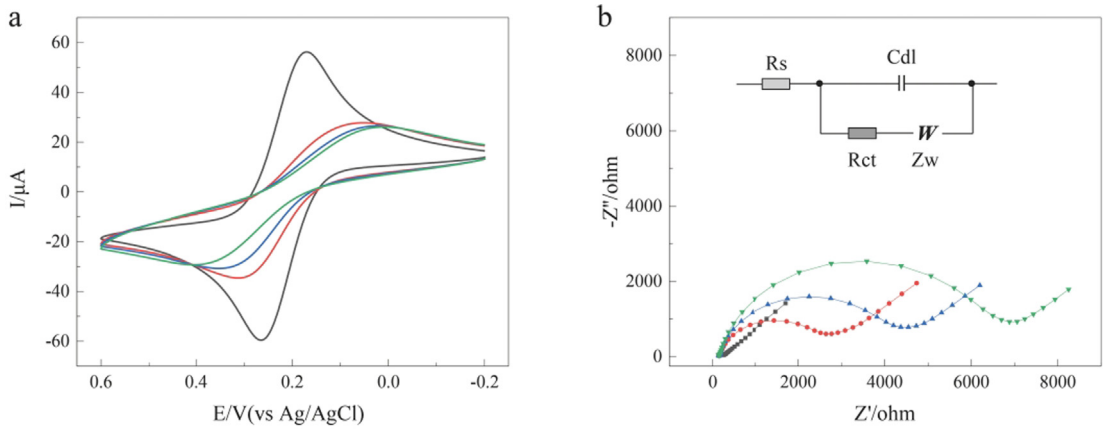

Fig. 2. Monitoring of biosensor fabrication. Cyclic voltammograms (a) and Nyquist plots (b) of bare Au electrode (black), the same electrode modified with 0.5 μM of peptide (Red), then conditioned in 10 mM of PBS (Blue), and after interacting with L-Arg (Green) were measured to confirm the successful self-assembly. The CV and EIS measurements were conducted in 10 mM of PBS in which 10 mM $[Fe(CN)6]^{3-/4-}$ (1:1) was used as electrochemical reporter with 0.1 M of KCl.

due to the covalently bonded peptides hindering electron transfer. This confirmed the successful self-assembly of the biosensor. The *R*ct further increased after the sensor was conditioned in PBS for 30 min, which can be attributed to the peptide folding to its native conformation. To eliminate this interference caused by the PBS solvent, in subsequent experiments the response was measured after interacting with PBS so that the folded peptide served as the baseline. The interaction of L-Arg with the peptide immobilized on the gold surface led to an increase in EIS intensity, which can be attributed to a binding-induced conformational change resulting in decreased electron transfer efficiency [51].

3.3. Time optimization

The performance of a sensor highly depends on the incubation time, as this has an important effect on both the sensitivity and efficiency [28]. In this study, we optimized the response time in two aspects, the duration for which the peptide was immobilized on the electrode and the interaction time between L-Arg and the modified electrode. To optimize the peptide immobilization time, equal volumes of peptide (7 μL, 0.5 μM) were dropped onto the pre-treated electrode surfaces and the electrodes were left for 1, 2, 4, and 6 h, respectively, at room temperature, maintaining a

high-humidity atmosphere to avoid liquid evaporation. As soon as the scheduled time was reached, the peptide-modified electrodes were washed gently with deionized water and conditioned in PBS for 30 min to allow the peptides to fold to their native conformation. Then, the EIS spectra were recorded. The results showed that the *R*ct values continually increased until 4 h, then reached a plateau and remained constant from 4 h to 6 h (Fig. 3a). This indicates that 4 h is sufficient time for the modified electrode to reach an equilibrium state, with EIS registering an *R*ct peak value of approximately 5000 Ω. Thus, 4 h was used in subsequent experiments.

To optimize the binding time between L-Arg and the peptide-modified electrode, the fabricated sensor was allowed to interact with equal volumes of L-Arg (1 μM, 7 μL) for different time periods (10, 20, 30, 40 and 50, min). Afterwards, the sensor was gently washed with deionized water to remove unbonded L-Arg, and CV and EIS were conducted. As shown in Fig. 3b, the output signal increased sharply at 10–30 min, which indicated that large amounts of L-Arg were entrapped by this sensor as revealed by the rise in *R*ct. At 40–50 min, *R*ct continued to rise but more slowly, increasing by only ~10%. As time efficiency is important in the determination of the target, and the signal showed only a minor increase after 30 min, this was identified as the optimal incubation time for rapid detection and was selected for subsequent experiments.

3.4. Detection performance of the aptasensor

A sensor for performance testing was then fabricated under the optimized conditions, that is, 5 mM of TCEP was used to condition the 0.5 μM peptide (7 μL) and the time for peptide immobilization was 4 h. Then, different concentrations of L-Arg were analyzed with the sensor for 30 min, in which EIS was recorded as the response signal. The results showed that with increasing L-Arg concentration, *R*ct continually increased, which can be attributed to the interaction between the peptide aptamer and L-Arg altering the conformation of the immobilized peptide on the electrode surface. This conformational change amplified the steric hindrance of the peptide and blocked some of the potential binding sites, both of which suppressed electron transfer [52]. The electrochemical biosensor achieved a good response to L-Arg at concentrations ranging from 0.1 pM to 0.1 mM, which completely covered the L-Arg concentrations found in tissues (Fig. 4). The values of Δ*R*ct (=$R_{Arg} - R_{PBS}$) were used to fit a linear curve. The resulting curve confirmed a good correlation between Δ*R*ct and the logarithm of L-Arg concentration, where the linear equation was

$$y = 704.5log(c) + 11329.0, R^2 = 0.9925, \quad (a)$$

in which *c* was the concentration of L-Arg. The limit of detection (LOD) was calculated to be 1.1×10^{-15} mol L^{-1} using the equation LOD = 3 × σ/S, where σ is the standard deviation and S is the slope of the linear equation. This indicates that the designed sensor based on a peptide is sufficiently sensitive for L-Arg detection. Compared with previous L-Arg sensors, the fabricated electrochemical biosensor is more sensitive, with a wider range of detection and lower LOD (Table 2). It is interesting that, a discrepancy was found between the K_d values measured by ITC and EIS. This can be ascribed to two causes: first, when performing ITC verification, the temperature was maintained at 37 °C for consistency with the docking simulations, while electrochemical detection was performed at room temperature (25 °C); second, the concentration of ligand used in ITC may also have partly influenced K_d [53], although this may only have played a minor role.

3.5. Anti-interference detection

To verify whether this peptide-based biosensor has the specific ability to recognize L-Arg without interference by similar molecules, we tested the output signal of L-Arg in the presence of interferents. Equal concentrations of L-Arg and amino acid interferents (1 μM) including L-Tyr, L-Trp, L-Thr, L-Pro, L-Lys, L-His, L-Asp, L-Ser, L-Asn, L-Gln, L-Glu, L-Phe, L-Met, L-Cys, L-Ala, L-Ile, L-Leu, L-Gly, and L-Val were analyzed separately with the biosensor, and the responses of the modified biosensor were recorded. To clearly visualize the signal changes caused by the interferents, the data were normalized. As illustrated in Fig. 5, relative signal changes of 10% to 18% were caused by L-Ala, L-Cys, L-Glu, L-Gln, L-Asn, and L-Ser, while the other amino acids had negligible influences. These results indicate that this peptide aptamer-based biosensor possesses good selectivity, although the presence of some interference calls for further optimization.

3.6. Practical application

To test the feasibility of this sensor in real samples, pig serum samples were collected and then centrifuged at 3000 rpm for 10 min and stored at −80 °C until use. Before the experiment, the defrosted pig serum was diluted 100-fold with PBS, then L-

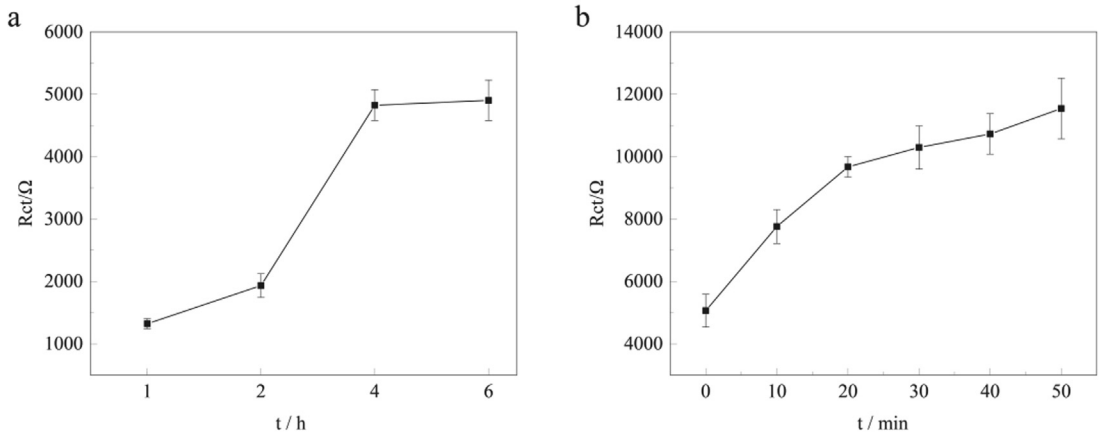

Fig. 3. Time optimization of the biosensor based on the peptide. (a) Incubation time of the peptide and gold electrode, using 7 μL of 0.5 μM peptide. (b) Incubation time of L-Arg and the modified electrode, using 1 μM L-Arg to interact with the modified electrode. *R*ct was determined as the response signal of EIS, which was measured in 10 mM of PBS using 10 mM $[Fe(CN)6]^{3-/4-}$ (1:1) as the electrical reporter. The error bars represent that the measurements were conducted with three different electrodes.

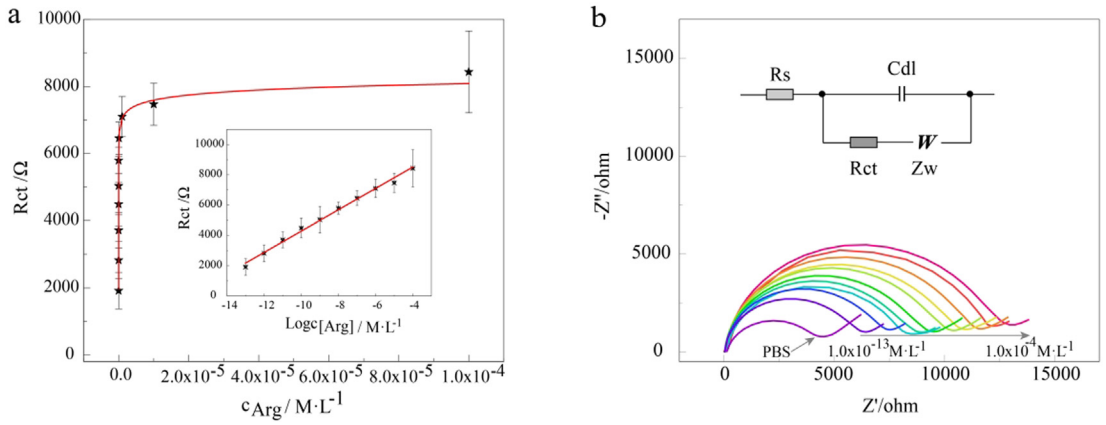

Fig. 4. Response of the aptasensor to different concentrations of L-Arg. EIS spectra was measured in 10 mM $[Fe(CN)6]^{3-/4-}$ (1:1) with 0.1 M of KCl, and the incubation between L-Arg and modified electrodes lasted for 30 min; the error bars in (a) represent that the measurements were obtained with three different electrodes, Nyquist plots (b) obtained for different concentration of L-Arg in PBS. The regression equation was y = 704.5log(c) + 11329.0, R^2 = 0.9925, c was the concentration of L-Arg.

Table 2
Comparison of current L-Arg sensors.

Signal	Recognition element	LOD	Linear range	Reference
Amperometric	Arginine deiminase	0.001 mM	0.003–0.2 mM	[54]
Fluorescent	Aptamer	1.8×10^{-9} M	2.5×10^{-8}–4×10^{-7} M	[40]
Phosphorescent	Arginine deiminase	/	1.0–10^{-4} M	[55]
Amperometric	Arginase	0.085 mM	0.15–0.6 M	[56]
Fluorescent	Arginine deiminase	0.25 μM	0.35 μM–24 μM	[57]
Fluorescent	Urease/arginase	0.082 mM	0.1–1.0 mM	[18]
EIS	Peptide aptamer	0.01 pM	0.1 pM–0.1 mM	Current work

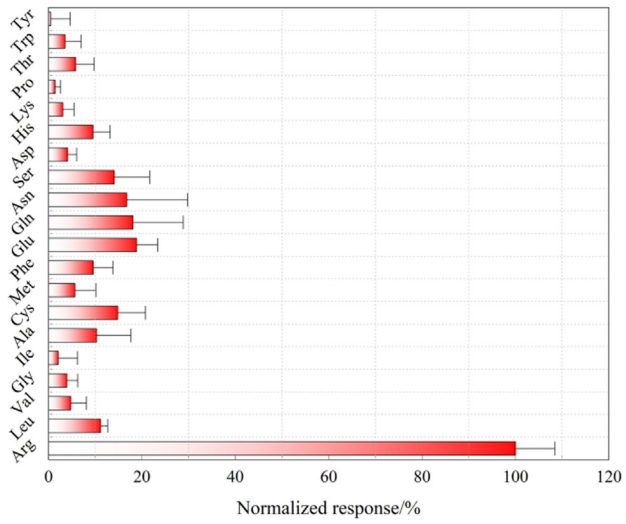

Fig. 5. Anti-interference capacity of the peptide-based biosensor. L-Arg and interferent amino acids were tested in equal concentrations, and the Δ*R*ct values were normalized (Normalized response = $\Delta Rct_{AA}/\Delta Rct_{Arg} \times 100\%$). The error bars represent the data were measured by three different electrodes.

Arg in high concentration (10 mM) was spiked into the diluted pig serum to prevent significant volume change. The successfully fabricated biosensors were used to detect L-Arg according to the method described above, that is, 7 μL of diluted serum spiked with 0.2 μM of L-Arg was dropped onto the PBS-conditioned electrode and incubated for 30 min; then, after washing with deionized water, the EIS spectra were recorded to calculate the corresponding L-Arg concentration through Eq. (a). As shown in Table 3, satisfactory detection results were obtained by the modified electrode, in which the calculated recovery rates were between 96.9% and 104.4%, and the RSD was less than 4.0%. This indicated that the peptide-based biosensor gave a reliable result compared with HPLC. Compared with HPLC, one advantage of this peptide aptamer-based biosensor is that it avoids amino acid derivatization. Additionally, it may be possible to integrate the biosensor into a portable electrochemical workstation to allow fast detection in real-life scenarios where experimental equipment is limited.

4. Conclusion

In this study, we demonstrated that docking was an effective tool to screen peptide aptamers for amino acid-binding capacity,

Table 3
Detection of real L-Arg samples by modified electrode.

Serum no.	HPLC (μM)	Spiked (μM)	Found (μM)	RSD (%)	Recovery rate (%)
Serum 1	0.2170	0.2000	0.4257 ± 0.0150	4.01	104.4
Serum 2	0.2121	0.2000	0.4058 ± 0.0245	−3.00	96.9
Serum 3	0.2457	0.2000	0.4494 ± 0.0163	1.50	101.7
Serum 4	0.3601	0.2000	0.5583 ± 0.0055	−0.01	99.1
Serum 5	0.2999	0.2000	0.4959 ± 0.0070	−1.33	98.0

Note: RSD was calculated by RSD = (Found − Spiked − HPLC)/HPLC × 100%, recovery rate was calculated by recovery rate = (Found − HPLC)/Spiked × 100%, Found is represented as Mean ± SD (*n* = 3).

the veracity of which was experimentally confirmed by ITC. The chosen peptide was modified and then used as the recognition element for biosensor fabrication, as the target amino acid (L-Arg) induced a conformational change in the peptide. On this basis, we designed an EIS-based biosensor for L-Arg detection. This novel sensor showed an acceptable performance in that the linear range was 0.1 pM–0.1 mM and the LOD was 0.01 pM. Anti-interference experiments and analysis of real pig serum samples further validated the feasibility of this sensor. However, more efforts are needed to improve the specificity and accuracy in real samples. In conclusion, this study provides a new strategy to conduct peptide screening and biosensor fabrication for biological molecules.

Declaration of Competing Interest

The authors declare that they have no known competing financial interests or personal relationships that could have appeared to influence the work reported in this paper.

Acknowledgement

This work was supported by National Key Scientific Instrument and Equipment Development Projects of China (free application) (31527803).

Authors' contributions

ZF and ZC conceived and designed the experiments. ZF and LD performed the peptide aptamer scale simulate screening. YH performed the ITC experiment, YH and LZ performed the electrochemical experiments. YH analyzed the data. ZF, ZC and YY contributed reagents/materials/analysis tools. YH and ZF drafted the article. All authors approved the submission.

Declaration of Competing Interest

The authors declare that they have no known competing financial interests or personal relationships that could have appeared to influence the work reported in this paper.

Appendix A. Supplementary material

Supplementary data to this article can be found online at https://doi.org/10.1016/j.bioelechem.2020.107634.

References

[1] P.E. Hall, R. Lewis, N. Syed, R. Shaffer, J. Evanson, S. Ellis, M. Williams, X. Feng, A. Johnston, J.A. Thomson, A Phase I study of pegylated arginine deiminase (pegargiminase), cisplatin and pemetrexed in argininosuccinate synthetase 1-deficient recurrent high-grade glioma, Clin. Cancer Res. 25 (2019) 2708–2716, https://doi.org/10.1158/1078-0432.CCR-18-3729.

[2] P.J. Popovic, H.J. Zeh, J.B. Ochoa, Arginine and Immunity, J. Nutr. 137 (2007) 1681–1686, https://doi.org/10.1093/jn/137.6.1681S.

[3] M.P. McRae, Therapeutic Benefits of L-arginine: an umbrella review of meta-analyses, J. Chiropractic Med. 15 (2016) 184–189, https://doi.org/10.1016/j.jcm.2016.06.002.

[4] L. Moren, R. Perryman, T. Crook, J.K. Langer, K. Oneill, N. Syed, H. Antti, Metabolomic profiling identifies distinct phenotypes for ASS1 positive and negative GBM, Bmc Cancer 18 (2018) 16, https://doi.org/10.1186/s12885-018-4040-3.

[5] C.N. Hinrichs, M. Ingargiola, T. Kaubler, S. Lock, A. Temme, A. Kohn-Luque, A. Deutsch, O. Vovk, O. Stasyk, L.A. Kunz-Schughart, Arginine deprivation therapy: putative strategy to eradicate glioblastoma cells by radiosensitization, Mol. Cancer Ther. 17 (2018) 393–406, https://doi.org/10.1158/1535-7163.mct-16-0807.

[6] C. Riess, F. Shokraie, C.F. Classen, B. Kreikemeyer, T. Fiedler, C. Junghanss, C. Maletzki, Arginine-depleting enzymes – an increasingly recognized treatment strategy for therapy-refractory malignancies, Cell. Physiol. Biochem. 51 (2018) 854–870, https://doi.org/10.1159/000495382.

[7] J. Szefel, A. Danielak, W.J. Kruszewski, Metabolic pathways of L-arginine and therapeutic consequences in tumors, Adv. Med. Sci. 64 (2019) 104–110, https://doi.org/10.1016/j.advms.2018.08.018.

[8] J. Suliburska, P. Bogdanski, M. Szulinska, D. Pupek-Musialik, A. Jablecka, Changes in mineral status are associated with improvements in insulin sensitivity in obese patients following L-arginine supplementation, Eur. J. Nutr. 53 (2014) 387–393, https://doi.org/10.1007/s00394-013-0533-7.

[9] J. Rodrigues-Krause, M. Krause, I.M.G. da Rocha, D. Umpierre, A.P.T. Fayh, Association of L-arginine supplementation with markers of endothelial function in patients with cardiovascular or metabolic disorders: a systematic review and meta-analysis, Nutrients 11 (2019) 18, https://doi.org/10.3390/nu11010015.

[10] M.G. Fleszar, J. Wiśniewski, M. Krzystek-Korpacka, B. Misiak, D. Frydecka, J. Piechowicz, K. Lorenc-Kukuła, A. Gamian, Quantitative analysis of L-arginine, dimethylated arginine derivatives, L-citrulline, and dimethylamine in human serum Using liquid chromatography-mass spectrometric method, Chromatographia 81 (2018) 911–921, https://doi.org/10.1007/s10337-018-3520-6.

[11] C.M. Ensor, F.W. Holtsberg, J.S. Bomalaski, M.A. Clark, Pegylated arginine deiminase (ADI-SS PEG20,000 mw) inhibits human melanomas and hepatocellular carcinomas in vitro and in vivo, Cancer Res. 62 (2002) 5443–5450.

[12] J. Fuhrmann, A. Schmidt, S. Spiess, A. Lehner, K. Turgay, K. Mechtler, E. Charpentier, T. Clausen, McsB is a protein arginine kinase that phosphorylates and inhibits the heat-shock regulator CtsR, Science 324 (2009) 1323–1327, https://doi.org/10.1126/science.1170088.

[13] O. Hodek, T. Krizek, P. Coufal, H. Ryslava, Design of experiments for amino acid extraction from tobacco leaves and their subsequent determination by capillary zone electrophoresis, Anal. Bioanal. Chem. 409 (2017) 2383–2391, https://doi.org/10.1007/s00216-017-0184-2.

[14] C.F. Qin, P. Huang, K. Qiu, W.J. Sun, L. Xu, X. Zhang, J.D. Yin, Influences of dietary protein sources and crude protein levels on intracellular free amino acid profile in the longissimus dorsi muscle of finishing gilts, J. Anim. Sci. Biotechnol. 6 (2015) 10, https://doi.org/10.1186/s40104-015-0052-x.

[15] M.M. Tian, J.F. Zhang, A.C. Mohamed, Y.Z. Han, L.P. Guo, L. Yang, Efficient capillary electrophoresis separation and determination of free amino acids in beer samples, Electrophoresis 35 (2014) 577–584, https://doi.org/10.1002/elps.201300416.

[16] Y.T. Song, C. Xu, H. Kuroki, Y.Y. Liao, M. Tsunoda, Recent trends in analytical methods for the determination of amino acids in biological samples, J. Pharm. Biomed. Anal. 147 (2018) 35–49, https://doi.org/10.1016/j.jpba.2017.08.050.

[17] M. Asal, O. Ozen, M. Sahinler, I. Polatoglu, Recent developments in enzyme, DNA and immuno-based biosensors, Sensors 18 (2018) 16, https://doi.org/10.3390/s18061924.

[18] K. An, H.D. Duong, J.I. Rhee, Ratiometric fluorescent L-arginine and L-asparagine biosensors based on the oxazine 170 perchlorate-ethyl cellulose membrane, Eng. Life Sci. 17 (2017) 847–856, https://doi.org/10.1002/elsc.201700033.

[19] Z.L. Chen, Q. He, M.M. Zhao, C.Y. Lin, F. Luo, Z.Y. Lin, G.N. Chen, A fluorometric histidine biosensor based on the use of a quencher-labeled Cu(II)-dependent DNAzyme, Microchim. Acta 184 (2017) 4015–4020, https://doi.org/10.1007/s00604-017-2425-7.

[20] Z. Cao, W.F. Li, C. Liu, Y.Y. Peng, Y. Huang, Z.L. Xiao, Design and fabrication of embedded wireless monitoring system based on bluetooth low energy transmission for potentiometric sensors, Chin. J. Anal. Chem. 47 (2019) 229–236, https://doi.org/10.19756/j.issn.0253-3820.181684.

[21] C.Z. Lv, Y. Xun, Z. Cao, J.L. Xie, D. Li, G. Liu, L. Yu, Z.M. Feng, Y.L. Yin, S.Z. Tan, Sensitive determination of toxic clenbuterol in pig meat and pig liver based on a carbon nanopolymer composite, Food Anal. Methods 10 (2017) 2252–2261, https://doi.org/10.1007/s12161-017-0796-3.

[22] Q. Zhu, C. Liu, L. Zhou, L. Wu, K.J. Bian, J.L. Zeng, J.X. Wang, Z.M. Feng, Y.L. Yin, Z. Cao, Highly sensitive determination of L-tyrosine in pig serum based on ultrathin CuS nanosheets composite electrode, Biosens. Bioelectron. 140 (2019) 175–182, https://doi.org/10.1016/j.bios.2019.111356.

[23] W.C. White, G.G. Guilbault, Lysine specific enzyme electrode for determination of lysine in grains and foodstuffs, Anal. Chem. 50 (1978) 1481–1486, https://doi.org/10.1021/ac50033a025.

[24] N. Verma, A.K. Singh, M. Singh, L-arginine biosensors: a comprehensive review, Biochem. Biophys. Rep. 12 (2017) 228–239, https://doi.org/10.1016/j.bbrep.2017.10.006.

[25] B.C.C. Pessela, G. Dellamora-Ortiz, L. Betancor, M. Fuentes, J.M. Guisán, R. Fernandez-Lafuente, Modulation of the catalytic properties of multimeric β-galactosidase from E. coli by using different immobilization protocols, Enzyme Microb. Tech. 40 (2007) 310–315, https://doi.org/10.1016/j.enzmictec.2006.04.015.

[26] C. Mateo, J.M. Palomo, G. Fernandez-Lorente, J.M. Guisan, R. Fernandez-Lafuente, Improvement of enzyme activity, stability and selectivity via immobilization techniques, Enzyme Microb. Technol. 40 (2007) 1451–1463, https://doi.org/10.1016/j.enzmictec.2007.01.018.

[27] N. Arroyo-Curras, J. Somerson, P.A. Vieira, K.L. Ploense, T.E. Kippin, K.W. Plaxco, Real-time measurement of small molecules directly in awake, ambulatory animals, PNAS 114 (2017) 645–650, https://doi.org/10.1073/pnas.1613458114.

[28] S.H. Baek, M.W. Kim, C.Y. Park, C.S. Choi, S.K. Kailasa, J.P. Park, T.J. Park, Development of a rapid and sensitive electrochemical biosensor for detection of human norovirus via novel specific binding peptides, Biosens. Bioelectron. 123 (2019) 223–229, https://doi.org/10.1016/j.bios.2018.08.064.

[29] S. Reverdatto, D.S. Burz, A. Shekhtman, Peptide aptamers: development and applications, Curr. Top. Med. Chem. 15 (2015) 1082–1101, https://doi.org/10.2174/1568026615666150413153143.
[30] A.B. Kinghorn, L.A. Fraser, S.L. Liang, S.C.C. Shiu, J.A. Tanner, Aptamer bioinformatics, Int. J. Mol. Sci. 18 (2017) 22, https://doi.org/10.3390/ijms18122516.
[31] Y. He, Y. Su, L. Hong, Z. Xiao, Z. Cao, Z. Feng, Y. Yin, Screening and application of peptamers, Scientia Sinica Vitae 48 (2018) 1054–1064, https://doi.org/10.1360/n052018-00024.
[32] Z.J. Zhuo, Y.Y. Yu, M.L. Wang, J. Li, Z.K. Zhang, J. Liu, X.H. Wu, A.P. Lu, G. Zhang, B.T. Zhang, Recent advances in SELEX technology and aptamer applications in biomedicine, Int. J. Mol. Sci. 18 (2017) 19, https://doi.org/10.3390/ijms18102142.
[33] A. Tripathi, V.A. Bankaitis, Molecular docking: from lock and key to combination lock, J. Mole. Med. Clin. Appl. 2 (2017), https://doi.org/10.16966/2575-0305.106.
[34] W.P. Hu, J.V. Kumar, C.J. Huang, W.Y. Chen, Computational selection of RNA aptamer against angiopoietin-2 and experimental evaluation, Biomed. Res. Int. 2015 (2015) 658712, https://doi.org/10.1155/2015/658712.
[35] Y.W. Cheung, J. Kwok, A.W. Law, R.M. Watt, M. Kotaka, J.A. Tanner, Structural basis for discriminatory recognition of Plasmodium lactate dehydrogenase by a DNA aptamer, PNAS 110 (2013) 15967, https://doi.org/10.1073/pnas.1309538110.
[36] A.B. Hashkavayi, J.B. Raoof, Ultrasensitive and reusable electrochemical aptasensor for detection of tryptophan using of Fe(bpy)(3) (p-CH3C6H4SO2) (2) as an electroactive indicator, J. Pharm. Biomed. Anal. 163 (2019) 180–187, https://doi.org/10.1016/j.jpba.2018.10.006.
[37] E. Omidinia, N. Shadjou, M. Hasanzadeh, Aptamer-based biosensor for detection of phenylalanine at physiological pH, Appl. Biochem. Biotechnol. 172 (2014) 2070–2080, https://doi.org/10.1007/s12010-013-0656-6.
[38] A. Geiger, P. Burgstaller, H. vonderEltz, A. Roeder, M. Famulok, RNA aptamers that bind l-arginine with sub-micromolar dissociation constants and high enantioselectivity, Nucl. Acids Res. 24 (1996) 1029–1036, https://doi.org/10.1093/nar/24.6.1029.
[39] K. Harada, A.D. Frankel, Identification of 2 novel arginine binding DNAs, EMBO J. 14 (1995) 5798–5811, https://doi.org/10.1002/j.1460-2075.1995.tb00268.x.
[40] H. Yuan, Y. Huang, J. Yang, Y. Guo, X. Zeng, S. Zhou, J. Cheng, Y. Zhang, An aptamer-based fluorescence bio-sensor for chiral recognition of arginine enantiomers, Spectrochim. Acta Part A Mol. Biomol. Spectrosc. 200 (2018) 330–338, https://doi.org/10.1016/j.saa.2018.04.038.
[41] J.S. Daniels, N. Pourmand, Label-free impedance biosensors: opportunities and challenges, Electroanalysis 19 (2007) 1239–1257, https://doi.org/10.1002/elan.200603855.
[42] Y. Li, M. Zhao, H. Wang, Label-free peptide aptamer based impedimetric biosensor for highly sensitive detection of TNT with a ternary assembly layer, Anal. Bioanal. Chem. 409 (2017) 6371–6377, https://doi.org/10.1007/s00216-017-0576-3.
[43] E. Mervinetsky, I. Alshanski, Y. Hamo, L.M. Sandonas, A. Dianat, J. Buchwald, R. Gutierrez, G. Cuniberti, M. Hurevich, S. Yitzchaik, Copper induced conformational changes of tripeptide monolayer based impedimetric biosensor, Sci. Rep. 7 (2017) 9498, https://doi.org/10.1038/s41598-017-10288-z.
[44] J. Wu, J.P. Park, K. Dooley, D.M. Cropek, A.C. West, S. Banta, Rapid development of new protein biosensors utilizing peptides obtained via phage display, PLoS ONE 6 (2011) e24948, https://doi.org/10.1371/journal.pone.0024948.
[45] W.L. DeLano, PyMOL: An Open-Source Molecular Graphics Tool, 2002. www.ccp4.ac.uk/newsletters/newsletter40/11_pymol.pdf.
[46] D.S. Goodsell, G.M. Morris, A.J. Olson, Automated docking of flexible ligands: applications of AutoDock, J. Mol. Recognit. 9 (1996) 1–5, https://doi.org/10.1002/(SICI)1099-1352(199601)9:13.0.CO;2-6.
[47] H. Rana, P. Moussatche, L.S. Rocha, S. Abdellaoui, S.D. Minteer, E.W. Moomaw, Isothermal titration calorimetry uncovers substrate promiscuity of bicupin oxalate oxidase from Ceriporiopsis subvermispora, Biochem. Biophys. Rep. 5 (2016) 396–400, https://doi.org/10.1016/j.bbrep.2016.01.016.
[48] J.L. Duan, J. Yin, W.K. Ren, T. Liu, Z.J. Cui, X.G. Huang, L. Wu, S.W. Kim, G. Liu, X. Wu, G.Y. Wu, T.J. Li, Y.L. Yin, Dietary supplementation with L-glutamate and L-aspartate alleviates oxidative stress in weaned piglets challenged with hydrogen peroxide, Amino Acids 48 (2016) 53–64, https://doi.org/10.1007/s00726-015-2065-3.
[49] S. Wang, J.H. Liu, Y.Y. Dong, H.J. Su, T.W. Tan, Conformational structure-dependent molecular recognition of two aptamers for tetracycline, RSC Adv. 5 (2015) 53796–53801, https://doi.org/10.1039/c5ra08050a.
[50] L. Baranauskiene, T.C. Kuo, W.Y. Chen, D. Matulis, Isothermal titration calorimetry for characterization of recombinant proteins, Curr. Opin. Biotechnol. 55 (2019) 9–15, https://doi.org/10.1016/j.copbio.2018.06.003.
[51] B.R. Baker, R.Y. Lai, M.C.S. Wood, E.H. Doctor, A.J. Heeger, K.W. Plaxco, An electronic, aptamer-based small-molecule sensor for the rapid, label-free detection of cocaine in adulterated samples and biological fluids, J. Am. Chem. Soc. 128 (2006) 3138, https://doi.org/10.1021/ja056957p.
[52] A.K. Yagati, A. Go, S.G. Chavan, C. Baek, M.H. Lee, J. Min, Nanostructured Au-Pt hybrid disk electrodes for enhanced parathyroid hormone detection in human serum, Bioelectrochemistry 128 (2019) 165–174, https://doi.org/10.1016/j.bioelechem.2019.04.011.
[53] W.H. Ward, G.A. Holdgate, Isothermal Titration Calorimetry in Drug Discovery, Progress in Medicinal Chemistry, Elsevier, 2001, pp. 309–376.
[54] M.T. Zhybak, L.Y. Fayura, Y.R. Boretsky, M.V. Gonchar, A.A. Sibirny, E. Dempsey, A.P.F. Turner, Y.I. Korpan, Amperometric L-arginine biosensor based on a novel recombinant arginine deiminase, Microchim. Acta 184 (2017) 2679–2686, https://doi.org/10.1007/s00604-017-2290-4.
[55] N. Verma, A.K. Singh, N. Saini, Synthesis and characterization of ZnS quantum dots and application for development of arginine biosensor, Sens. Bio-Sens. Res. 15 (2017) 41–45, https://doi.org/10.1016/j.sbsr.2017.07.004.
[56] N.Y. Stasyuk, G.Z. Gayda, M.V. Gonchar, L-Arginine-selective microbial amperometric sensor based on recombinant yeast cells over-producing human liver arginase I, Sens. Actuators, B 204 (2014) 515–521, https://doi.org/10.1016/j.snb.2014.06.112.
[57] N.Y. Stasyuk, G.Z. Gayda, L.R. Fayura, Y.R. Boretskyy, M.V. Gonchar, A.A. Sibirny, Novel arginine deiminase-based method to assay L-arginine in beverages, Food Chem. 201 (2016) 320–326, https://doi.org/10.1016/j.foodchem.2016.01.093.